



Original scientific paper

EDTA as a corrosion inhibitor for Al in 0.5 M HCl: adsorption, thermodynamic and theoretical study

Rehab E. Azooz✉

Chemistry Department, Faculty of Science, Jazan University, 2097 Jazan, Saudi Arabia

✉Corresponding Author: re_azooz@yahoo.com; Tel.: +9966532324115

Received: May 21, 2016; Revised: June 18, 2016; Accepted: July 4, 2016

Abstract

In this study; EDTA is used in very small amount (10^{-10} M) as an inhibitor for the Al corrosion in 0.5 M HCl. Thermodynamic and adsorption parameters are calculated. The result shows that, in this range of concentrations, EDTA is chemisorbed at the Al surface, forming a stable complex with Al and give inhibition efficiency up to 89 %. For more concentration, unstable complex is formed and acceleration of corrosion occurs. The adsorption fit well to Langmuir, Temkin isotherms and El-awady model. Density functional theory (DFT) is used to study the geometrical optimizations of EDTA. From the obtained optimized structure, The highest occupied molecular orbital (E_{HOMO}), the lowest unoccupied molecular orbital (E_{LUMO}) and their energy difference (ΔE), the total energy (TE), electronegativity (χ), dipole moment (μ), global hardness (η), global softness (σ), electron affinity (A), ionization potential (I), the fraction of electrons transferred (ΔN) and were determined using B3LYP/6-31G(d,p) basis set.

Keywords

EDTA; Inhibition efficiency; Adsorption isotherms; Thermodynamic parameters; Theoretical parameters

Introduction

The study of Al corrosion is of great importance; various industrial operations depend mainly on Al. Most investigations on the corrosion of Al have been carried out on. The development of corrosion inhibitor is a good branch based on a functional organic compound. The structure and function groups of used organic compounds are useful for obtaining a good inhibitors [1-4]. Depending upon excellent conductivity (electrically and thermally) of Al; application of Al is varied and widespread. [5]. Adsorption of inhibitor on the charged metal surface is the main process to inhibit corrosion, on this basis; multiple bond(s), an electron rich atom as, S, N or P or a ring is a

main centers for the adsorption processes. In aqueous media, inhibitors are used to prevent or reduce the corrosion of metals [6–11]. It was shown that, compounds containing N or/and O atoms exhibit a good inhibiting effect. A polyprotic acid, *i.e.* Ethylenediaminetetraacetic acid (EDTA), with a lone pair of electrons in its amino groups and two carboxylic acid groups is used for complexation with the charged metal ions [6,12]. Complexation occur between (free or π)-electrons from inhibitor and the vacant d-orbital of a metal through the formation of donor–acceptor surface [6,14-16]. In the last years, EDTA has been studied to protect metals from corrosion in different environments [16–19], it was found that, different parameter affects the inhibition effect of EDTA including, the pH value, temperature, concentration, and type of the metal. Nahle [20] has found that the Sn(II)–EDTA complex increased the dissolution rate of Sn in a basic medium. Milošev *et al.* [16] have investigated the corrosion of stainless steel in physiological solutions, while, EDTA prevents the formation of a passive layer and increases the solubility of the metal. Gadiyar *et al.* [22] have discovered that EDTA inhibits the corrosion of carbon steel. However, its inhibiting effect is imperfect. Alhaji and Reda [23] have stated that EDTA is effective in decreasing the corrosion rate of copper-nickel alloy in seawater contaminated with sulfur. S. Zor *et al.* [24] observe that, the corrosion of Al is higher in 0.1 M NaCl solution in higher concentration of EDTA, and become slower at 10^{-4} M EDTA

The molecular structure, electronic structure and reactivity of Inhibitors are determined well by quantum chemical methods [25]. A powerful framework is provided by DFT [25,26] that help in understanding a lot of chemical processes [27-31]. Concepts as, electronegativity hardness or softness *etc.* are used to describe chemical reactivity [28], are appear naturally within DFT. The local electron density/population displacements represented the inflow of a single electron is measured using Fukui function [30] and is representing the relative local softness of the electron gas. In the present study the inhibition effect of EDTA for the corrosion of Al in 0.5 M HCl has been done using both weight loss and electrochemical methods. The temperature effect and adsorption isotherms will be studied in details. Also analyzing the inhibitive properties of EDTA using DFT calculations will be done.

Experimental

Chemical and reagents

Al strips have a rectangular form (4.5×3.5×0.2 cm), with the composition 99.11 % of Al, 0.019 % of Zn, 0.036 % of Cu, 0.001 % of Mg, 0.834 % of Si and, were mechanically polished using different grades of emery sheets, washed with acetone and distilled water and dried. EDTA disodium salt (Analar grade) and HCl were obtained from Fluka AG, Switzerland. All solutions were prepared using freshly prepared bidistilled water. Stock solution of EDTA was prepared, from which all used concentrations are prepared via dilution.

Methods

Weight loss measurements

The Al samples (coupons) were weighed before immersion in 250 ml beaker containing 50 ml of the respective prepared test solutions at room temperature and desired temperatures. The setups were exposed for a period of 100 min. Corrosion reaction is quenched in concentrated HNO_3

digressed in CH_3COCH_3 washed under water, dried and weighed. A mean value triplicate experiments is reported in each case. The values of weight loss in the presence and the absence of EDTA is used to calculate efficiency at the end of definite intervals of time.

Temperatures effects

The same procedure adopted where the temperature of the study was varied, in the range (303-333 K), from at the end of each experiment. The specimens were taken out, washed both in running tap water and into distilled water. They were dried and their weights were recorded.

The loss in weight was calculated. Each experiment was duplicated to get good reproducibility. Weight loss measurement was performed in 0.5 M HCl with and without the addition of EDTA in the range $(6.4 - 10.07) \times 10^{-10}$ M.

Electrochemical methods

All electrochemical experiments were recorded using a potentiostat/galvanostat (EG&G 326A, U.S.A). The potential was scanned at the scan rate 10 mV s^{-1} . All experiments were repeated to ensure reproducibility. Fresh solution was used for each experiment. The cell used is a three compartment home-made one, with a reference saturated calomel electrode (SCE), an auxiliary (Pt-foil) electrode and a working (Al) electrode with 0.4 cm^2 area exposed to corroded solution was used.

Adsorption isotherms

The adsorption of inhibitor at a metal /solution interface is the main source of inhibition effect, accordingly, the isotherms of adsorption can be determined. In order to obtain the isotherm the fractional surface coverage values (θ) as a function of inhibitor concentration must be obtained. The values of θ can be easily determined from the weight loss measurements by the ratio;

$$\theta = \frac{I.E.}{100}$$

where IE is inhibition efficiency obtained by a weight loss method. So, it is necessary to determine empirically which isotherm fits best to the adsorption of inhibitor on the Al surface.

Scanning electron microscopy (SEM)

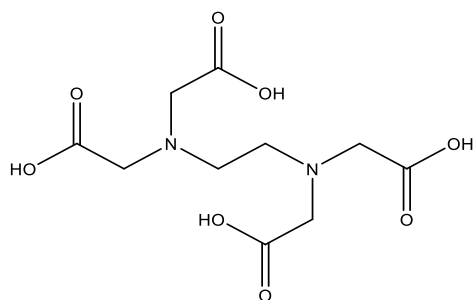
After a period of 100 min, Al coupons was removed from solution, rinsed with a double distilled water, dried and observed in a Scanning Electron Microscope (JSM-T20 Electron Probe Micro-analyzer (JEOL, Tokyo, Japan)) to examine the surface morphology. The following cases were examined, to understand the morphology of the Al surface in the absence and presence of inhibitors, (i) aluminum coupon after polishing, (ii) aluminum coupon dipped in 0.5 M HCl for 100 min. at 303 K and (iii) aluminum coupon dipped in 0.5 M HCl containing 2.7×10^{-10} M of EDTA inhibitor 100 min

Quantum chemical calculations

DFT is used to obtain the complete geometrical optimizations of EDTA, with Beck's exchange functional along with nonlocal correlation functional (B3LYP) of Lee–Yang–Parr [32–34] with 6-31G* basis set in Gaussian 03 program package [35]. From the obtained optimized structure, several quantum chemical parameters were calculated; E_{HOMO} , E_{LUMO} , ΔE_{gap} , the dipole μ and TE .

Results and discussion

The molecular structure of an organic compound used in the present study is given in Scheme 1.



Scheme 1. Structure of EDTA

Open circuit potential

Potential-time curves were recorded for 60 minutes of immersion of the Al specimens in aqueous 0.5 M HCl solution without and with EDTA at required concentrations. As seen in Figure 1. From Figure 1, when Al is immersed in the HCl solution E_{OCP} drops sharply, then began to increase to more positive value and reached a stationary value after 25 minutes of immersion. The aggressiveness of the corroded solution may cause the differences in E_{OCP} values at the beginning of Al exposure, It was suggested that, adsorption of EDTA molecules on the Al surface is the reason for the initial negative shift.

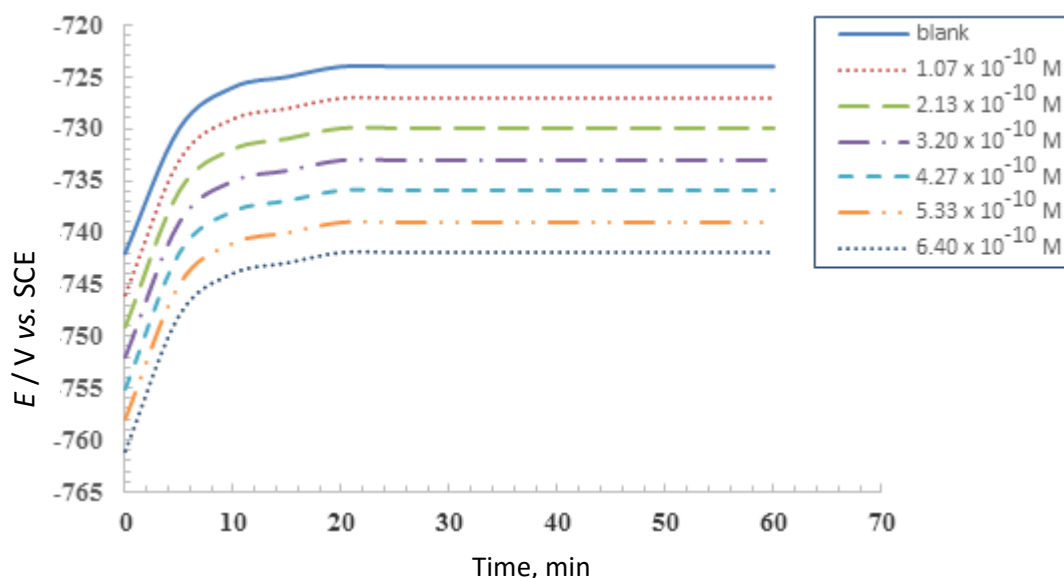


Figure 1. Potential - time curves for Al in 0.5 M HCl in absence and presence of different concentrations of (EDTA) at 303 K.

The results have shown that the addition of EDTA molecules at the beginning shifts E_{OCP} to more negative values. And then become more positive with time, due to oxide film growth [36]. In particular, initial values are more negative than steady state values, also the dependence of the E_{OCP} on concentration suggests that, the inhibitor molecules are strong and rapidly adsorbed at the steady state potentials [36].

Potentiodynamic polarization studies

The cathodic and anodic polarization curves of Al in 0.5 M HCl in the absence and presence of different EDTA concentrations at 303 K are shown in Fig. 2. The electrochemical kinetic parameters

(in the potential range ± 50 mV from E_{corr}), namely, corrosion current (i_{corr}), corrosion potential (E_{corr}), and Tafel slopes, (β_c and β_a), have been determined simultaneously and are listed in Table 1. Data infer that, the addition of EDTA to the acid solutions increases both the anodic and cathodic overpotentials, decreases the corrosion current density, i_{corr} , and shifts the E_{corr} to more positive values. This means that the presence of EDTA inhibits the partial anodic dissolution of Al and also retards the partial cathodic reduction of hydrogen ion.

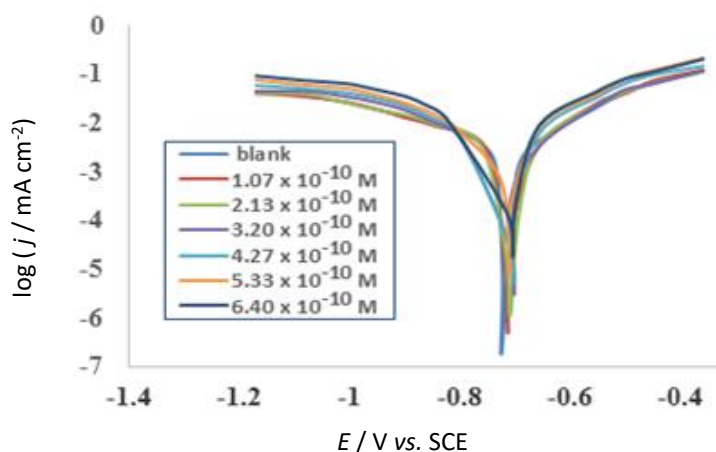


Figure 2. Potentiodynamic polarization curves for Al in 0.5M HCl at 303 K with scan rate of 10 mV s^{-1} with and without different concentrations of EDTA.

These results reveal that EDTA acts as a mixed type inhibitor. The inhibition efficiency IE , at different inhibitor concentrations at 303 K for Al electrode in 0.5 M HCl solution was calculated from the Equation 1 [37-39]:

$$IE / \% = \left(1 - \frac{i_{\text{corr}}}{i_{\text{corr}}^0} \right) \times 100 \quad (1)$$

where, i_{corr}^0 and i_{corr} are corrosion current density for uninhibited and inhibited solutions respectively.

Table 1. The electrochemical kinetic parameters (i_{corr} , E_{corr} , β_c and β_a) and inhibition efficiency (IE) obtained from polarization curves of Al electrode in 0.5M HCl at 303 K in the absence and the presence of EDTA.

$C_{\text{EDTA}} / \text{M}$	$i_{\text{corr}} / \text{mA cm}^{-2}$	$-E_{\text{corr}} / \text{mV}$	$-\beta_c / \text{mV dec}^{-1}$	$-\beta_a / \text{mV dec}^{-1}$	$IE / \%$
Blank	0.89	670	122	0.69	--
$1.07 \cdot 10^{-10}$	0.47	660	118	0.60	47.2
$2.13 \cdot 10^{-10}$	0.46	650	116	0.53	48.3
$3.20 \cdot 10^{-10}$	0.35	630	118	0.52	60.7
$4.27 \cdot 10^{-10}$	0.21	580	112	0.51	76.4
$5.33 \cdot 10^{-10}$	0.12	530	115	0.50	86.5
$6.40 \cdot 10^{-10}$	0.10	500	114	0.50	88.8

Mass loss

The mass losses of Al in 0.5 M HCl solution, with and without different concentrations of the EDTA were recorded after 100 min. of immersion at different temperatures. The corrosion rates of Al alloy were calculated using Equation 2 [37].

$$CR = \frac{87.6 \Delta m}{Atd} \quad (2)$$

where Δm is the mass lost (g), 87.6 is a constant, A is the surface area of the coupon (cm^2), d is the density (g cm^{-3}), t is the time of exposure (h). The calculated CR fits into the range (less than $0.50 \text{ mm year}^{-1}$) at which the application is acceptable [39]. Figure 3 (A and B) shows the variation in mass loss for Al coupons in the absence and the presence of EDTA. The mass loss in the presence of inhibitor is much smaller than the blank solution. The significant difference shows reduce impact on the CR of Al in 0.5 M HCl.

Both of the surface coverage (θ) and the inhibition efficiency (IE) were calculated using mass loss data according to Equations 3 and 4, respectively [38].

$$\theta = \left(1 - \frac{w_{inh}}{w_{blank}} \right) \tag{3}$$

$$IE / \% = \theta \times 100 \tag{4}$$

where, w_{blank} is the corrosion rate in the uninhibited environments. w_{inh} is the corrosion in the inhibited environment. The high inhibition efficiency as the inhibitor concentration increases could be understood to be due to the reduction in corrosion rate. Thus, EDTA could be considered as an inhibitor of Al in 0.5 M HCl solution given the high level of inhibition efficiency. The inhibitor efficiency, increased with the inhibitor concentration.

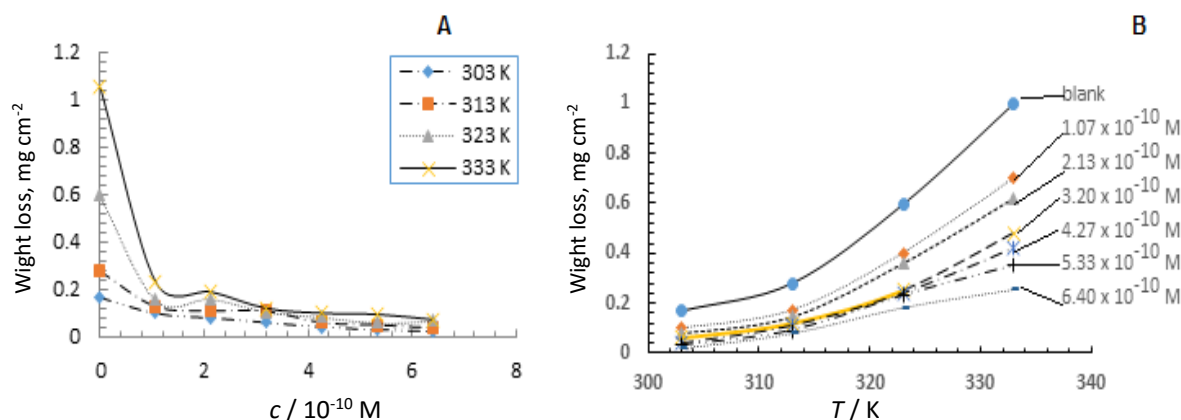


Figure 3. Mass loss of Al immersed for 100 min. in 50ml HCl in the presence or absence of EDTA at different temperatures and EDTA concentrations.

Figure 4 shows the inhibition efficiency in different concentration of the EDTA and it is seen that the IE increases linearly with the inhibitor concentration.

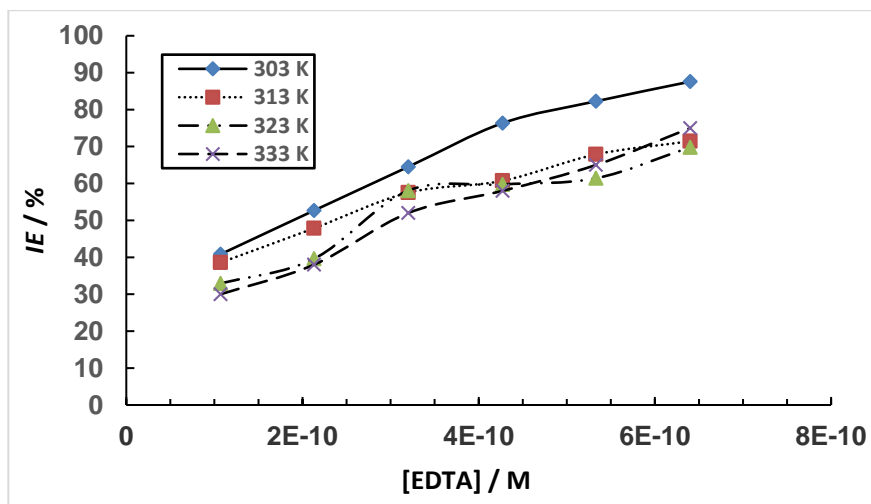


Figure 4. IE after 100 min. in 50 ml HCl at different [EDTA] at different temperatures

Adsorption studies

Inhibition efficiencies of Al in 0.5 M HCl was increase with increasing additive concentrations of EDTA, this phenomenon can be explained on the basis of adsorption. Adsorption of the inhibitor can explain the nature of Al/EDTA interaction. In the acid solution, firstly inhibitor is adsorbed on the metal surface and cover certain area from corroded solution and decrease or prevent this area from dissolution, whereas corrosion reactions normally occurred on inhibitor-free areas. Accordingly, the area covered with inhibitor species (θ), can follow as a function of inhibitor concentration and/or solution temperature. When θ is tested as a function of the concentration (at constant temperature), the adsorption isotherm can be evaluated at the equilibrium condition. Four adsorption isotherms were tested using data from both weight loss and electrochemical techniques;

A. Langmuir's isotherm

The dependence of θ at the concentration of the inhibitor, was fitted to Langmuir's isotherm, assuming that, a fixed number of adsorption sites is present on Al surface, each one of these sites holds only one adsorbed species. Figure 5 shows linear plots of c/θ versus c with $R^2 \geq 0.90$, the average correlation coefficient, which suggests that adsorption was fitted to Langmuir's isotherm as in Equation 5 [37].

$$\frac{c}{\theta} = \frac{1}{K_{\text{ads}}} + c \quad (5)$$

where c is inhibitor concentration, K_{ads} adsorptive equilibrium constant representing the degree of adsorption (*i.e.* if K_{ads} having higher value, the inhibitor is strongly adsorbed on metal surfaces).

As shown in Table 2, the value of K_{ads} which was obtained from the reciprocal of the intercept of a Langmuir plot lines, and R^2 of all lines were near unity. This means that obtained results is fit well with Langmuir isotherm. The higher values of K_{ads} indicating a strong interaction between EDTA and the Al surface. It seemed, therefore, that electrostatic interaction (physisorption) between inhibitor molecules existing as cations should prevail over molecular interaction, and this often results in strong interactions (chemisorption).

Table 2. Data obtained from Figure 3

Temperature, K	303		313		323		333	
Technique used*	Wt.-loss	Elec.	Wt.-loss	Elec.	Wt.-loss	Elec.	Wt.-loss	Elec.
R^2	0.99	0.93	0.99	0.96	0.98	0.97	0.98	0.97
$\Delta G^{\circ}_{\text{ads}}$, kJ mol ⁻¹	-66.38	-66.38	-67.25	-70.95	-70.78	-70.76	-71.83	-75.16

* Wt.-loss - Weight loss measurements; Elec. - Electrochemical methods

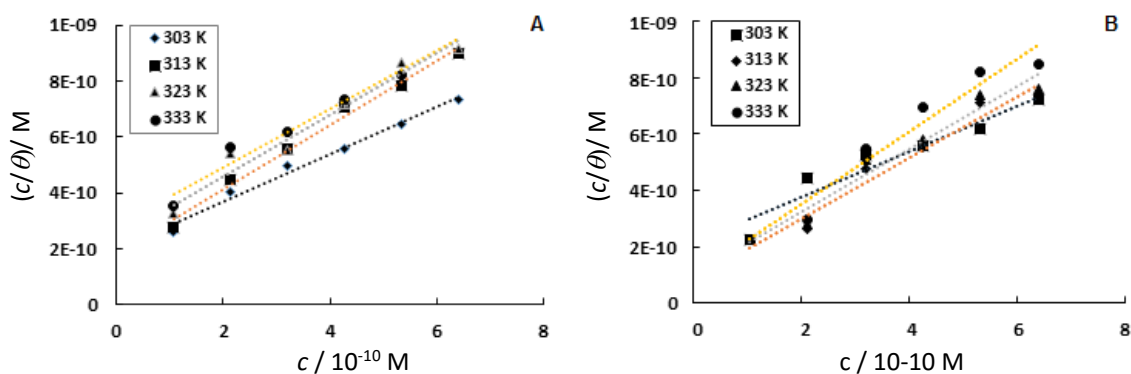


Figure 5. Plots of c/θ versus c of Langmuir's adsorption isotherm for the corrosion of Al in 0.5 M HCl at different temperatures. A: From weight loss technique and B: from electrochemical technique

The Equilibrium constant of adsorption K_{ads} is related to the standard adsorption free energy (ΔG^0_{ads}) by Equation 6:

$$K_{ads} = \frac{1}{55.5} \exp\left(-\frac{\Delta G^0_{ads}}{RT}\right) \tag{6}$$

where 55.5 is the concentration of water in the solution expressed in, R is the gas constant and T is the absolute temperature. From Table 1, the average value of standard adsorption free energy (ΔG^0_{ads}) > -40 kJ mol⁻¹. The negative value of ΔG^0_{ads} ensures spontaneity of the adsorption process and the stability of the adsorbed layer on metal surfaces. In general, the values of (ΔG^0_{ads} up to -20 kJ mol⁻¹ are consistent with the electrostatic interaction between the charged molecules and the charged metal (physisorption), while those around -40 kJ mol⁻¹ or higher are associated with chemisorption as a result of sharing or transferring of electrons from organic molecules to metal surface to form a coordinate type of bond. In the present work, the calculated value of ΔG^0 in all studied temperatures in both techniques are > -40 kJ mol⁻¹ indicating that the adsorption mechanism of EDTA on Al surfaces in 0.5 M HCl solution was typical of chemisorptions.

B. Temkin isotherm

The nature of the interaction at metal/solution interface is studied by Temkin isotherm. By assuming a uniform distribution of the adsorption energy that increases with the increase of the θ . Temkin isotherm model are given by the Equation (7a and 7b).

$$\exp(f, \theta) = K_{ads}c \tag{7a}$$

and it is rearranged

$$\theta = (1/f) \log c + (1/f) \log K_{ads} \tag{7b}$$

where K_{ads} is the equilibrium constant, c is the inhibitor concentration, θ is the surface coverage, f is the interaction term parameter, a lateral attraction between the adsorbing molecules is assumed if $f > 0$, but if $f < 0$, there is a lateral repulsion. The plot of θ versus $\log c$, yields curve with linear correlation coefficient $R^2 \geq 0.90$, close to unity, in all cases. The obtained value of K_{ads} (average) $\approx 4.1 \times 10^4$ and $\approx 4.4 \times 10^4$ in case of weight loss and polarization techniques repetitively, $f > 0$ indicating a strong lateral attraction between the adsorbing molecules of EDTA and the surface of the Al.

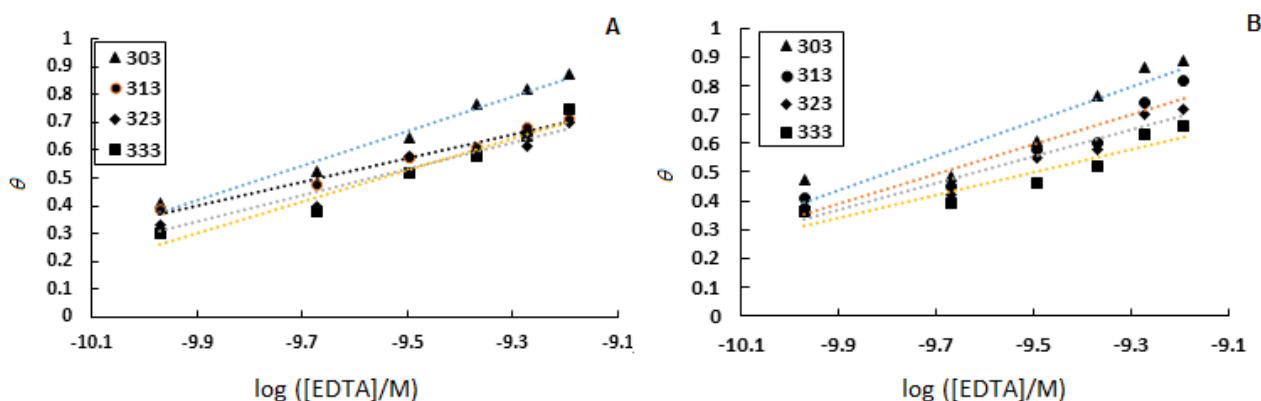


Figure 6. Plots of θ versus $\log c$ of Temkin’s adsorption isotherm for the corrosion of Al in 0.5 M HCl at different temperatures, A: from weight loss technique and B: from electrochemical technique

Table 3. Data obtained from Figure 4

T / K	303		313		323		333	
Technique used*	Wt.-loss	Elec.	Wt.-loss	Elec.	Wt.-loss	Elec.	Wt.-loss	Elec.
<i>f</i>	1.6	1.7	2.3	1.93	2.1	2.15	1.8	2.49
K_{ads}	3.9×10^4	4.1×10^4	5.1×10^4	4.2×10^4	4.1×10^4	4.4×10^4	3.3×10^4	4.7×10^4
R^2	0.95	0.90	0.96	0.90	0.95	0.91	0.95	0.91

* Wt.-loss - Weight loss measurements; Elec. - Electrochemical methods

C. Flory-Huggins isotherm

The amount of the inhibitor molecules that could displace the water molecules from the metal surface is studied using Flory-Huggins isotherm, which is showed by equation. 8

$$\log(\theta/c) = \log k + x \log(1-\theta) \quad (8)$$

where x is the size parameter that measure the number of adsorbed water molecules replaced by a given inhibitor molecule. Figure 7 shows the plot of $\log(\theta/c)$ vs. $\log(1-\theta)$, linear relationships with $R^2 > 0.8$ is obtained, and indicating Flory-Huggins isotherm was obeyed. The obtained $(K_{ads})_{avg} = 1.5 \times 10^4$ and the calculated $\Delta G_{ads} > -34$ kJ/mol. The size parameter is approximately 1.

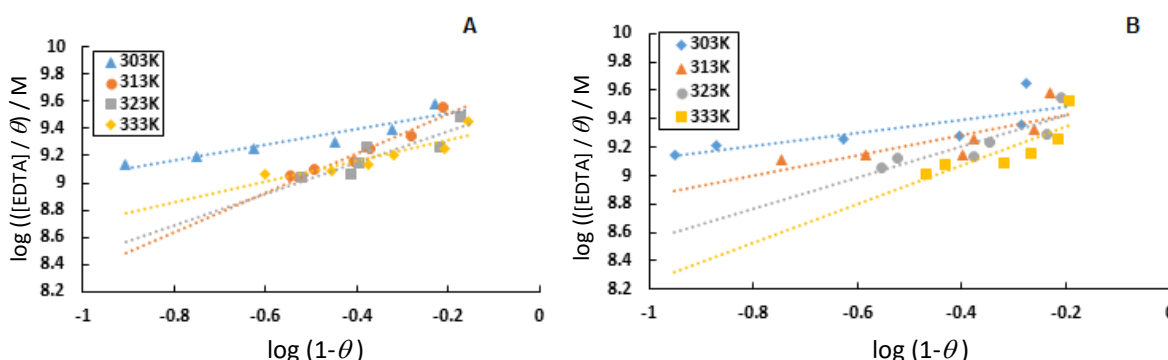


Figure 7. Plots of $\log(1-\theta)$ versus $\log(\theta/c)$ of Flory Huggin's adsorption isotherm for the corrosion of Al in 0.5 M HCl at different temperatures, A: From weight loss technique and B: from electrochemical technique

Table 4. Data obtained from Figure 5

T / K	303		313		323		333	
Technique used*	Wt.-loss	Elec.	Wt.-loss	Elec.	Wt.-loss	Elec.	Wt.-loss	Elec.
x	0.58	0.47	1.45	0.71	1.15	1.1	0.76	1.4
K_{ads}	1.5×10^4	1.5×10^4	1.8×10^4	1.4×10^4	1.5×10^4	1.5×10^4	1.3×10^4	1.5×10^4
R^2	0.96	0.90	0.98	0.90	0.95	0.91	0.95	0.91

* Wt.-loss - Weight loss measurements; Elec. - Electrochemical methods

D. Thermodynamic-kinetic model

The surface coverage values obtained from the gravimetric and polarization measurements were also fitted into the adsorption isotherm of the thermodynamic-kinetic model of El-Awady et al. are represented in Equation. 9

$$\log\left(\frac{\theta}{1-\theta}\right) = \log K'c + y \log c \quad (9)$$

where c is the concentration of the exudates, θ is the degree of surface coverage, K_{ads} is the Equilibrium constant of adsorption process, and $K_{ads} = K^{1/y}$. $1/y$ is the number of inhibitory molecules occupying one active site (or the number of water molecules replaced by one molecule of EDTA). Curves fitting of the data in the thermodynamic-kinetic model is shown in Fig. 8. This data gave straight lines, the values of $1/y$ and K_{ads} calculated from the El-Awady *et al.* curve model is given in

Table 4. The values of 1/y (average) obtained are more than unity in all cases, indicating that each molecule EDTA involved in the adsorption process is attached to more than one active site on the metal surface.

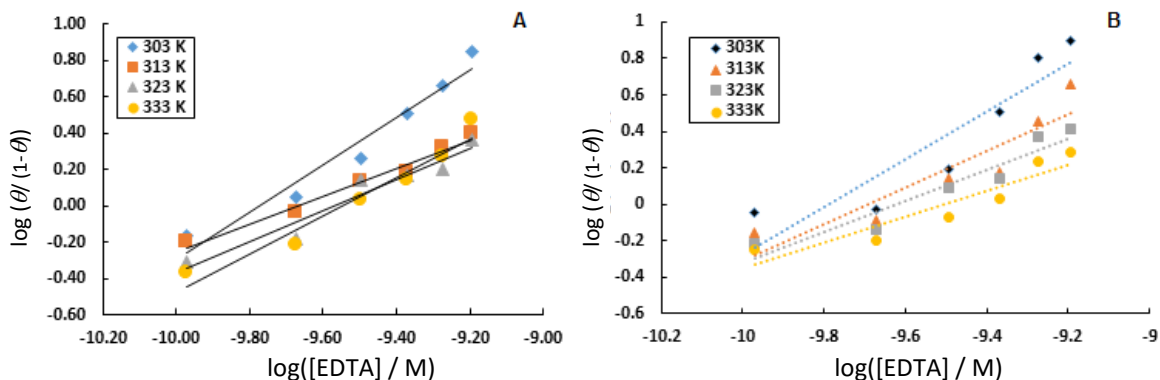


Figure 8. Plots of log c versus log (θ / 1-θ) of thermodynamic-kinetic model for the corrosion of Al in 0.5 M HCl at different temperatures, A: From weight loss technique and B: from electrochemical technique

Table 5. Data obtained from Figure 5

T / K	303		313		323		333	
Technique used*	Wt.-loss	Elec.	Wt.-loss	Elec.	Wt.-loss	Elec.	Wt.-loss	Elec.
y	1.31	1.32	0.77	1	0.86	0.84	1.05	0.72
1/y	0.77	0.76	1.31	1	1.22	1.18	0.92	1.39
K ¹	7.7 x10 ¹⁴	9.1x10 ¹⁴	4.1 x10 ¹²	3.7 x10 ¹³	8.9 x10 ¹²	7.9x 10 ¹²	5.3x 10 ¹³	2.1x10 ¹²
R ²	0.95	0.90	0.94	0.90	0.94	0.92	0.93	0.91

* Wt.-loss - Weight loss measurements; Elec. - Electrochemical methods

By rearrangement of Gibbs-Helmholtz equation we obtain Equation 10, which is used to calculate the enthalpy of adsorption (ΔH_{ads})

$$\Delta G_{ads}/T = (\Delta H_{ads}/T) K \tag{10}$$

A plot between the variations of (ΔG_{ads}/T) and (1/T) gave a straight line whose slope is ΔH_{ads} as shown in Figure 9. The entropy of adsorption ΔS_{ads} was calculated using the following thermodynamic Equation (Equation 11):

$$\Delta S_{ads} = (\Delta H_{ads} \Delta G_{ads}) / T \tag{11}$$

where, data of ΔG_{ads} were taken from Langmuir isotherm results (from its R² value, it is the best fit model)

The obtained date of the calculated ΔH_{ads} and ΔS_{ads} was tabulated in Table 6.

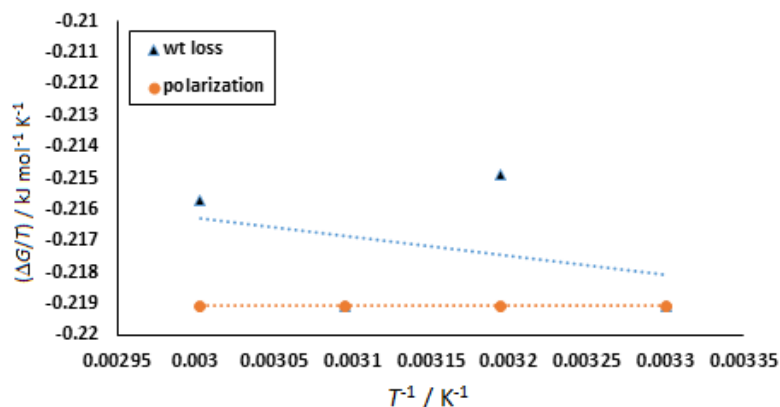


Figure 9. Gibbs-Helmholtz rearranged relation between (ΔG_{ads}/T) and (1/T)

Table 6. Adsorption thermodynamic parameters obtained using Langmuir isotherm

T / K	303		313		323		333	
Technique used*	Wt.-loss	Elec.	Wt.-loss	Elec.	Wt.-loss	Elec.	Wt.-loss	Elec.
$-\Delta G_{ads} / \text{kJ mol}^{-1}$	66.38	66.38	67.25	70.95	70.78	70.76	71.83	75.16
$-\Delta H_{ads} / \text{kJ mol}^{-1}$	6.02	0.02	6.02	0.02	6.02	0.02	6.02	0.02
$\Delta S_{ads} / \text{J mol}^{-1} \text{K}^{-1}$	199.2	196.1	195.6	203.7	200.4	196.1	197.6	202.7

* Wt.-loss - Weight loss measurements; Elec. - Electrochemical methods

The negative sign of ΔH_{ads} indicated the exothermic process of adsorption of the inhibitor on aluminum surface in HCl. The positive value of ΔS_{ads} in the presence of inhibitor can be attributed to the increase in the solvent entropy and more positive desorption entropy. It is also interpreted that the increase of disorderness is due to more water molecules which can be desorbed from the metal surface by one inhibitor molecule. Therefore, it is revealed that decrease in the enthalpy is the driving force for the adsorption of the inhibitor on the surface of aluminum [28,29]. The calculated values of heat of adsorption and entropy of adsorption are listed in Table (6).

Effect of temperature

Based on temperature effect, inhibitors may be classified into three groups:

1. Inhibitors whose inhibition efficiency (*IE*) decreases with temperature increase. The value of the apparent activation energy E_a , found is greater than that in the uninhibited solution;
2. Inhibitors in whose *IE* does not change with temperature variation. The apparent activation energy E_a , does not change with the presence or absence of inhibitors;
3. Inhibitors in whose presence the *IE* increases with temperature increase while the value of E_a for the process is smaller than that obtained in the uninhibited solution.

Thus, in examining the effect of temperature on the corrosion process in the presence of EDTA, the Arrhenius Equation (Eq. 12) is helpful

$$\log CR = \frac{-E_a}{2.303 RT} + \log A \quad (12)$$

where *CR* is the corrosion rate, E_a is the apparent activation energy, *R* is the molar gas constant, *T* is the absolute temperature, and *A* is the frequency factor. Figure 10 represents the Arrhenius plot as log *CR* vs. 1/*T* for Al corrosion in 0.5 M HCl in free so inhibited solution, linear plots were obtained. The values of E_a were obtained from the slope of the Arrhenius plot and are presented in Table 8. From the table, it is seen that E_a increases in the presence of the inhibitors compared to the blank. The higher value of the activation energy of the process in an inhibitor's presence when compared to that in its absence is attributed to its physisorption, while the opposite is the case with chemisorption.

According to Eyring relationships (Eq. 13), both of S^* and H^* could be obtained,

$$-\ln \frac{Rh}{NT} R_c = \frac{\Delta H^*}{RT} - \frac{\Delta S^*}{R} \quad (13)$$

where *h* is the Planck's constant (6.626176×10^{-34} J s), *N* is the Avogadro's number (6.02252×10^{23} mol⁻¹), *R* is the universal gas constant, ΔH is the enthalpy of activation and ΔS is the entropy of activation. The kinetic results were found to fit the Arrhenius and Eyring equation, where plots of 1/*T* vs. ln *Rc/T* or 1/*T* vs. $-\ln(hRc/k_B T)$ (k_B is Boltzman constant and equation the term *R/N*) resulted in good straight lines. The activation parameters ΔH^* and ΔS^* can be evaluated from the slopes and intercepts of the straight line.

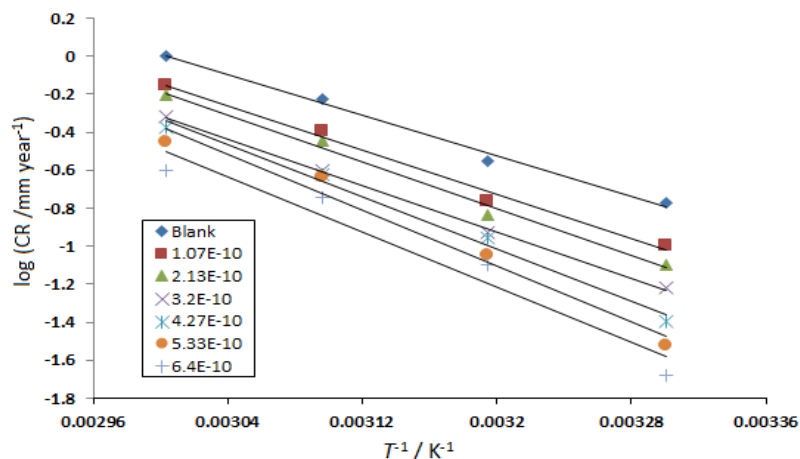


Figure 10. Arrhenius plot as log CR vs. 1/T for Al corrosion in 0.5 M HCl in the absence and presence of various concentrations of EDTA. Data obtained from weight loss technique

Table 7. Activation energy, E_a for aluminum corrosion in the presence of EDTA in 0.5 M HCl.

c / M	$-E_a / \text{kJ mol}^{-1}$
0	51.05
1.07×10^{-10}	56.01
2.13×10^{-10}	59.11
3.20×10^{-10}	58.55
4.27×10^{-10}	65.93
5.33×10^{-10}	70.02
6.40×10^{-10}	69.64

Figure 11 shows Eyring plot and all lines are straight from which ΔH and ΔS were evaluated and their values are put in Table 8.

The positive values of ΔH reflect the endothermic dissolution of Al in the presence and absence of the inhibitor. The increase in ΔH_a with the increase in the concentration of the inhibitor for Al corrosion reveals that, the decrease in Al corrosion rate is mainly controlled by kinetic parameters of activation. The negative values of ΔS may reflect the association mechanism of corrosion, *i.e.*, the decrease in disorder takes place on going from reactants to the activated state.

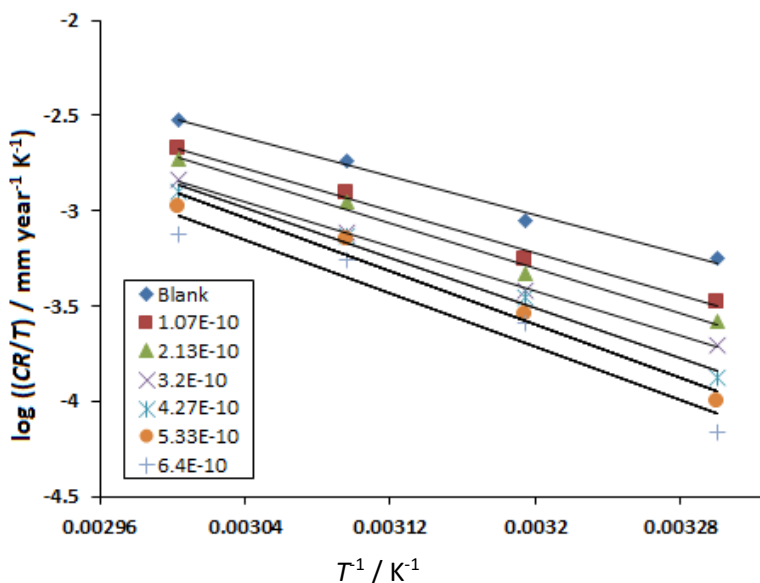


Figure 11. Eyring plot as log CR/T vs. 1/T for Al corrosion in 0.5 M HCl in the absence and presence of various concentrations of EDTA. Data obtained from weight loss technique

Table 8. Thermodynamic parameters, ΔH and ΔS
(for aluminum corrosion in the presence of EDTA in 0.5 M HCl)

c / M	$-\Delta S^* / J mol^{-1} K^{-1}$	$\Delta H^* / kJ mol^{-1}$
0	100.49	21.02
$1.07 \cdot 10^{-10}$	88.52	23.18
$2.13 \cdot 10^{-10}$	80.07	24.52
$3.20 \cdot 10^{-10}$	84.13	24.28
$4.27 \cdot 10^{-10}$	62.26	27.48
$5.33 \cdot 10^{-10}$	50.85	29.26
$6.40 \cdot 10^{-10}$	54.26	29.10

SEM

SEM analysis of Al metal surface, The SEM image of the aluminum specimen before and after immersing in 0.5M HCl for 100 min in the absence and presence of inhibitor system are shown in Figures 12 (A, B and C) repetitively. The SEM micrographs of aluminum surface after polishing (Fig. 8A) shows a smooth surface of the Al with no corrosion products on its surface. The SEM micrographs of the Al surface immersed in 0.5 M HCl (Fig. 12B) Shows its roughness which indicate the corrosion of Al in HCl. Fig. 12C indicates that in the presence of 10^{-10} M of EDTA, the surface coverage increases, which in turn results in the formation of insoluble complex on the surface of the metal (EDTA/inhibitor complex) and the surface is covered by a thin layer of inhibitor which effectively control the dissolution of aluminum.

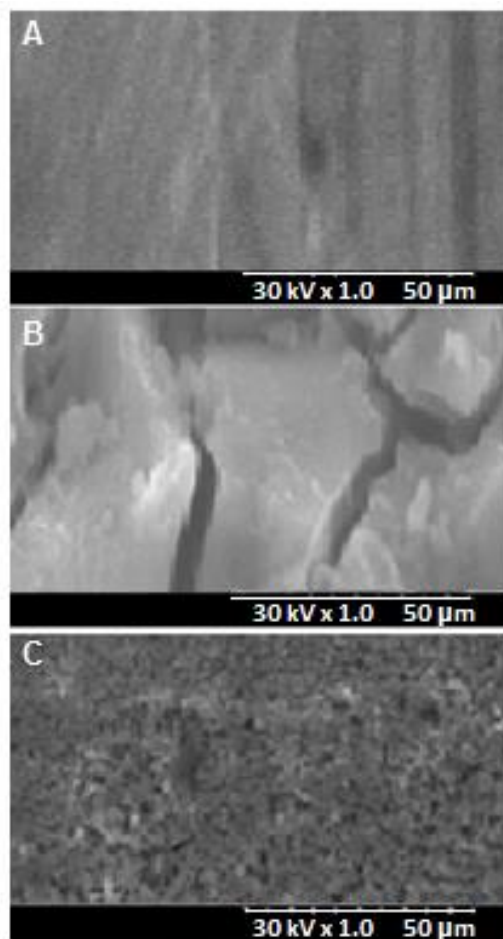


Figure 12. SEM of Al surface at 30 °C; A) After polishing, B) after immersion in 0.5 M HCl for 100 min., and C) the same as B but in the presence of $2.7 \cdot 10^{-10}$ M EDTA

Quantum chemical calculations

The activity properties of an inhibitor is related to its geometry as well as the nature of its Frontier Molecular Orbitals, FMO, namely, the HOMO and LUMO. Therefore, in this study, quantum chemical calculations were performed to investigate the relationship between molecular structure of this compound and their inhibition effect. The optimized molecular structure and the FMO density distribution of the studied molecule are shown in Figs. 13 and 14, and the calculated quantum chemical parameters are given in Table 9 .

Adsorption centers of the inhibitor molecules are predicted by FMO. These centers are responsible for the interaction with surface metal atoms [42,43]. It was reported that, inhibitors with high HOMO energy offering electrons to unoccupied d orbital of the metal. Where, inhibitors with lower LUMO energy accept electrons from metal surface, as the ΔE_g decreased, the efficiency of inhibitor improved [44]. The dipole moment (μ) of EDTA is 5.0542 Debye (1.69×10^{-29} C m), which is higher than that of H_2O ($\mu = 6.20 \times 10^{-30}$ C m = 1.856 Debye). The high value of μ probably increases the adsorption between EDTA and Al surface [45]. Accordingly, the adsorption of EDTA from the aqueous solution can be regarded as a quasi-substitution process between the EDTA in the aqueous phase [$EDTA_{sol}$] and water molecules at the electrode surface [H_2O_{ads}]. Analysis of Fig. 13 shows that the distribution of two energies HOMO and LUMO localized in the nitrogen and oxygen atoms, consequently this is the favorite sites for interaction with the metal surface. The total energy of the EDTA is equal to -691282.91 kcal mol $^{-1}$. This result indicated that EDTA is favorably adsorbed through the active centers of adsorption.

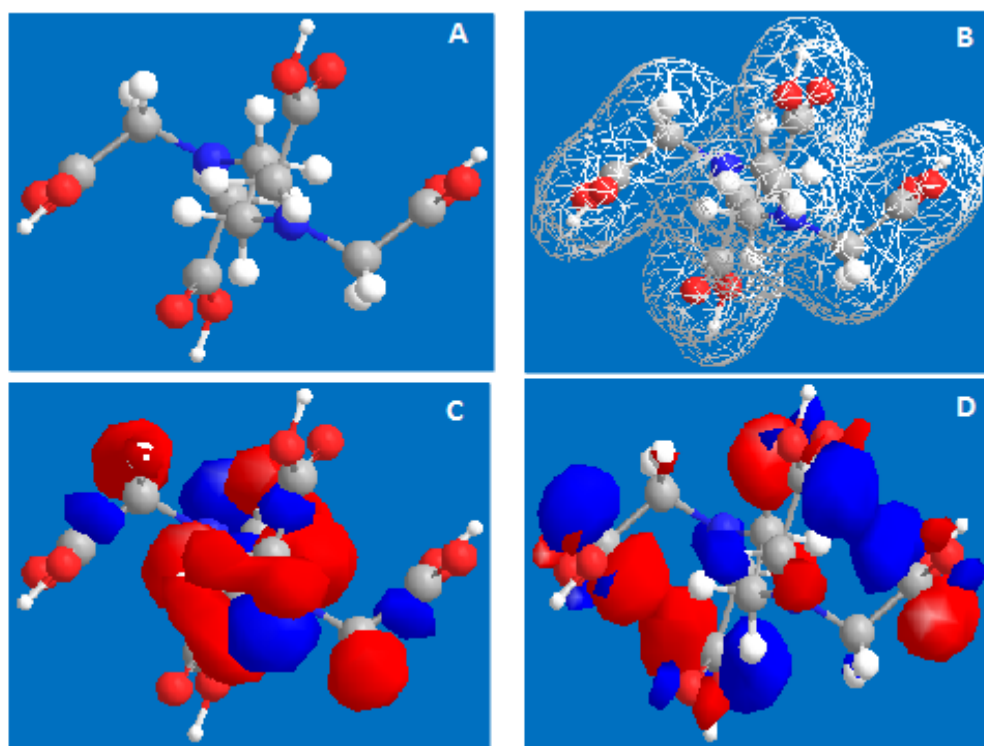


Figure 13. Optimized structure (A), total energy (B) Frontier molecular orbital diagrams; HUMO (C) and LUMO (D) of the EDTA by B3LYP/6-31G (d,p)

The number of transferred electrons (ΔN) was also calculated according to Eq. (14) [46,47]

$$\Delta N = \frac{\chi_{Al} - \chi_{EDTA}}{2(\eta_{Al} + \eta_{EDTA})} \quad (14)$$

Where χ_{Al} and χ_{EDTA} denote the absolute electronegativity of Al and EDTA molecule, respectively; η_{Al} and η_{EDTA} denote the absolute hardness of Al and EDTA molecule, respectively. These quantities are related to electron affinity (A) and ionization potential (I)

$$\chi = \frac{I + A}{2} \text{ and } \eta = \frac{I - A}{2}$$

where, I and A are related in turn to E_{HOMO} and E_{LUMO}

$$I = -E_{\text{HOMO}} \text{ and } A = -E_{\text{LUMO}}$$

Values of η_{EDTA} and χ_{EDTA} were calculated by using the values of I and A obtained from quantum chemical calculation. The theoretical values of χ_{Al} and η_{Al} are 3.230 and 2.77 eV mol⁻¹, respectively [46]. The fraction of electrons transferred from inhibitor to the iron molecule (ΔN) was calculated. According to other reports [46,47], value of ΔN showed inhibition effect resulted from electrons donation. Also the softness is calculated depending upon the following relation:

$$\sigma = 1/\eta$$

In this study, the EDTA was the donators of electrons while the Al surface was the acceptor. The EDTA was bound to the Al surface, and thus formed inhibition adsorption layer against corrosion.

The adsorption centers of EDTA are estimated by Mulliken population analysis [48]. Authors believe that, the heteroatom with more negatively charged, is adsorbed on the metal surface through the donor-acceptor type reaction [43].

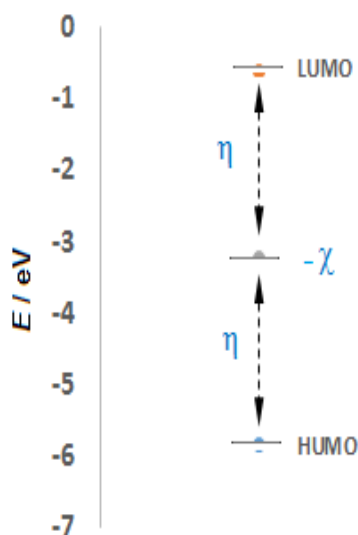


Figure 14. Energy distribution of EDTA using B3LYP/6-31G (d,p)

Table 9. Calculated quantum chemical data for EDTA by B3LYP/6-31G (d,p)

T.E. / kcal mol ⁻¹	$E_{\text{HOMO}} / \text{eV}$	$E_{\text{LUMO}} / \text{eV}$	$\Delta E_{\text{gap}} / \text{eV}$	μ / Debye	I / eV	A / eV	χ / eV	η / eV	σ / eV	$\Delta N / \text{eV}$
-691282.91	-5.849	-0.613	5.236	5.0542	5.849	0.613	3.231	2.618	0.382	-9.28x10 ⁻⁵

The Mulliken charge of EDTA was shown in Table 10. It can be seen that the most favorable sites for the interaction with the Al surface were the following atoms: N32, N24, N30, N13, O23, O31, O15 and O14. Because these atoms have larger negative charge, that donate electron. This being the preferred zone for nucleophilic attack. For EDTA, the HOMO is localized over the nitrogen N and oxygen O atoms, consequently this is the favorite sites for interaction with the metal.

Table 10. Mulliken charge of EDTA by B3LYP/6-31G (d,p)

Atom	Charge	Atom	Charge	Atom	Charge
1 C	0.214984	22 C	0.325515	43 H	0.121164
2 C	-0.086817	23 O	-0.567231	44 H	0.133160
3 C	-0.127361	24 N	-0.721935	45 H	0.133125
4 C	-0.144686	25 C	0.210742	46 H	0.140598
5 C	-0.066095	26 C	-0.010327	47 H	0.139131
6 C	0.015268	27 C	-0.083902	48 H	0.140004
7 C	0.216462	28 C	-0.148904	49 H	0.151805
8 C	0.040626	29 C	-0.123161	50 H	0.116621
9 C	-0.006822	30 C	0.326666	51 H	0.379970
10 C	0.000002	31 O	-0.567208	52 H	0.337115
11 C	-0.073095	32 N	-0.732883	53 H	0.147454
12 C	0.028970	33 C	0.185485	54 H	0.162757
13 N	-0.306615	34 C	0.001330	55 H	0.130880
14 O	-0.413216	35 C	-0.084377	56 H	0.379729
15 O	-0.419654	36 C	-0.146845	57 H	0.336862
16 N	-0.302210	37 C	-0.105158	58 H	0.154020
17 C	0.220038	38 C	0.388987	59 H	0.167164
18 C	-0.031616	39 O	-0.588086	60 H	0.137476
19 C	0.044560	40 N	-0.863854	61 H	0.351188
20 C	-0.021716	41 H	0.134813	62 H	0.302186
21 C	-0.140200	42 H	0.120365	63 H	0.346753

Conclusions

- EDTA acts as inhibitors for aluminum corrosion in acidic medium at very low concentrations 10^{-10} M.
- Inhibition efficiency of EDTA increases with increase in concentration of the inhibitors, but decreases with increase in temperature.
- The values of $\Delta G^{\circ}_{\text{ads}}$ are negative, which suggests that the inhibitors were strongly adsorbed on the Al surface. The values obtained support the chemisorption adsorption mechanism.
- EDTA is found to obey Langmuir, Temkin adsorption isotherm and kinetic-thermodynamic model of El-Awady et al for both weight loss and polarization techniques, from the fit of experimental data.
- Thermodynamic parameters revealed that the adsorption process is spontaneous.
- Quantum chemical parameters such as E_{HOMO} , E_{LUMO} , ΔE ($E_{\text{LUMO}} - E_{\text{HOMO}}$), dipole moment (μ), number of transferred electrons (ΔN), and total energy (TE) were found to give good correlation with experimentally determined inhibition efficiency

References

- [1] J. W. Diggle, T. C. Downie, C. W. Goulding, *Chem. Rev.* **65** (1969) 365-405
- [2] C. M. A. Brett, *J. Appl. Electrochem.* **20** (1990) 1000-1003
- [3] J. B. Bessone, D. R. Salinas, C. E. Mayer, W. J. Lorenz, *Electrochim. Acta.* **37** (1992) 2283-2290
- [4] G. R. T Schueller, S. R Taylor, E. E. Hajcsar, *J. Electrochem. Soc.* **139** (1992) 2799-2805
- [5] T. D. Burleigh, A. T. Smith, *J. Electrochem. Soc.* **138(8)** (1991) L34-L35
- [6] Q. Qu, S. Jiang, W. Bai, L. Li, *Electrochim. Acta* **52(24)** (2007) 6811-6820
- [7] E. M. Sherif, S. M. Park, *Electrochim. Acta* **51(22)** (2006) 4665-4673
- [8] M. A. Quraishi, R. Sardar, *Corrosion* **58(9)** (2002) 748-755
- [9] S. Zor, P. Doğan, B. Yazici, *Corros. Sci.* **47(11)** (2005) 2700-2710
- [10] S. Zor, P. Doğan, *Corros. Rev.* **22(3)** (2004) 209-217

- [11] S. Zor, *Turkish J. Chem.* **26(3)** (2002) 403-408
- [12] S. T. Selvi, V. Raman, N. Rajendran, *J. Appl. Electrochem.* **33(12)** (2003) 1175-1182
- [13] Y. K. Agrawal, J. D. Talati, M. D. Shah, *J. Appl. Electrochem.* **46(3)** (2004) 633-651
- [14] M. A. Quraishi, H. K. Sharma, *Mater. Chem. Phys.* **78(1)** (2003) 18-21
- [15] N. Ochoa, F., Moran N. Pebere, B. Tribollet, *Corros. Sci.* **47(3)** (2005) 593-604
- [16] G. M. Treacy, A. L. Rudd, C. B. Breslin, *J. Appl. Electrochem.* **30(6)** (2000) 675-683
- [17] N. S. Gaikwad, C. H. Bhosale, *Mater. Chem. Phys.* **76(2)** (2002) 198-203
- [18] L. R. B. Holzle, D. S. Azambuja, C. M. S. Piatnicki, G. E. Englert, *Mater. Chem. Phys.* **91(2-3)** (2005) 375-380
- [19] L. Di Palma, R. Mecozzi, *J. Hazard. Mater.* **147(3)** (2007) 768-775
- [20] A. Nahle, *Bull. Electrochem.* **14(2)** (1998) 52-56
- [21] I. Milošev, *J. Appl. Electrochem.* **32** (2002) 311-320
- [22] H. S. Gardiyar, N. S. D. Elayathu, *Corrosion* **36(6)** (1980) 306-312
- [23] J. N. Alhajji, M. R. Reda, *J. Electrochem. Soc.* **141(6)** (1994) 1432-1439
- [24] S. Zor, H. Ozkancanc, M. Bingul, *Mater. Sci.* **44(6)** (2008) 850-856
- [25] E. Kraka, D. Cremer, *J. Am. Chem. Soc.* **122 (2000)** 8245-8264
- [26] R. G. Parr, W. Yang, *Density Functional Theory of Atoms and Molecules*; Oxford University Press, New York, NY, USA, 1989
- [27] M. H. Cohen. *In Topics in Current Chemistry*; R. F. Nalewajski, Ed.; Springer-Verlag: Heidelberg, Germany, **183** (1996) 143-173
- [28] R.T Sanderson, *J. Am. Chem. Soc.* **74 (1952)** 272-274
- [29] M. K. Awad, *J. Electroanal. Chem.* **567** (2004) 219-225
- [30] R. G. Parr, W. Yang, *J. Am. Chem. Soc.* **106** (1984) 4049-4050
- [31] R. G. Pearson, *J. Am. Chem. Soc.* **85** (1963) 3533-3543
- [32] A. D. Becke, *J. Chem. Phys.*, **96** (1992) 9489-9502
- [33] A. D. Becke, *J. Chem. Phys.* **98** (1993) 1372-1377
- [34] C. Lee, W. Yang, R. G. Parr, *Phys. Rev. B* **37** (1988) 785-789
- [35] M. J. Frisch, *et al.*, *Gaussian 03, Revision B.01*, Gaussian, Inc., Pittsburgh, PA, USA, 2003.
- [36] F. El-Hajjaji, R. A. Belkhmima, B. Zerga, M. Sfaira, M. Taleb, M. Ebn Touhami, B. Hammouti, S. S. Al-Deyab, E. Ebenso, *Int. J. Electrochem. Sci.*, **9** (2014) 4721-4731
- [37] S. S. Abd El Rehim, S. M. Sayyah, M. M. El-Deeb, S. M. Kamal, R. E. Azooz, *Mater. Chem. Phys.* **123** (2010) 20-27
- [38] S. S. Abd El Rehim, S. M. Sayyah, R. E. Azooz, *Port. Electrochim. Acta* **30(1)** (2012) 67-80
- [39] D. William, Jr. Callister, *Materials Science and Engineering: an Introduction*, 7th edition, John Wiley & Sons, Inc., New York, NY, USA, 2007
- [40] B. Bouklah, M. Hammouti, F. L. Bentiss, *Corr. Sci.* **48(9)** (2006) 2831-2842
- [41] J. I. Bhat, D. P. Vijaya, *J. Korean Chem. Soc.* **55(5)** (2011) 835-841
- [42] J. Fang, J. Li, *J. Mol. Struct. THEOCHEM* **593** (2002) 179-185
- [43] G. Bereket, E. Hur, C. Og̃retir, *J. Mol. Struct. THEOCHEM* **578** (2002) 79-88
- [44] K.F. Khaled, *Appl. Surf. Sci.* **255** (2008) 1811-1818
- [45] K. Ramji, D.R. Cairns, S. Rajeswari, *Appl. Surf. Sci.* **254** (2008) 4483-4493
- [46] I. Lukovits, E. Kalman, F. Zucchi, *Corrosion* **57** (2001) 3-8
- [47] H. Ju, Z. Kai, Y. Li, *Corros. Sci.* **50** (2008) 865-871
- [48] M. Sahin, G. Gece, E.K. Arci, S. Bilgic, *J. Appl. Electrochem*, **382** (2008) 809-815

2016 by the authors; licensee IAPC, Zagreb, Croatia. This article is an open-access article distributed under the terms and conditions of the Creative Commons Attribution license (<http://creativecommons.org/licenses/by/4.0/>)